Investigative Radiology
Issue: Volume 33(11), November 1998, pp 810-821

Publication Type: [Original Investigations: Original Articles]
ISSN: 0020-9996
Accession: 00004424-199811000-00004
Keywords: Liposomal Gd-HP-DO3A, liposome, size, composition, liver contrast enhancement, dipolar relaxation, susceptibility effects

[Original Investigations: Original Articles]

Paramagnetic Liposomes as Magnetic Resonance Imaging Contrast Agents: Assessment of Contrast Efficacy in Various Liver Models

FOSSHEIM, SIGRID L. MSc Pharm*; COLET, JEAN-MARIE PhD+; MANSSON, SVEN MSc++; FAHLVIK, ANNE KJERSTI PhD*; MULLER, ROBERT N. PhD+; KLAVENESS, JO PhD*

Author Information

From the *Department of Medicinal Chemistry, School of Pharmacy, University of Oslo, Oslo, Norway; +NMR Laboratory, Department of Organic Chemistry, University of Mons-Hainaut, Mons, Belgium; ++Department of Experimental Research, Malmo University Hospital, University of Lund, Malmo, Sweden.
This work was supported by the Norwegian Research Council (contract 107462/410), Norwegian Pharmaceutical Society, BIOMED II MACE Program of the Commission of the European Community (contract BMH4CT-96-0051, DG12-SSMA), and the ARC Program (contract 95/00-194) of the French Community of Belgium.
Reprint requests: Sigrid L. Fossheim, Department of Medicinal Chemistry, School of Pharmacy, University of Oslo, PO Box 1155, Blindern, 0316 Oslo, Norway.
Received April 1, 1998, and accepted for publication, after revision, August 12, 1998.

Abstract

RATIONALE AND OBJECTIVES. Liposomal gadolinium (Gd)-HP-DO3A has been evaluated as a contrast agent for liver magnetic resonance imaging. The influence of various liposomal physicochemical properties on the liver uptake and contrast efficacy was investigated in various ex vivo and in vivo liver models.

METHODS. Liposomes of different size and membrane properties were prepared. The liposome size ranged from 74 to 304 nm. Two types of phospholipid compositions were studied; a mixture of hydrogenated phosphatidylcholine (HPC) and hydrogenated phosphatidylserine (HPS) with a phase transition temperature (T_m) of 51[degrees]C and, a blend composed of dipalmitoylphosphatidylcholine (DPPC) and dipalmitoylphosphatidylglycerol (DPPG) displaying a T_m of 41[degrees]C. Ex vivo tissue relaxometry and in vivo liver imaging were used to study the influence of liposome composition on the liver uptake and contrast efficacy of intravenously injected liposomes. The influence of liposome size and composition on the kinetics of liver uptake and imaging effect was assessed ex vivo in the perfused rat liver.

RESULTS. The HPC/HPS preparations showed generally a higher and faster liver uptake than the DPPC/DPPG preparations due to a higher stability in blood/perfusate (high T_m) and to the HPS component. The liposome size modulated the extent and kinetics of liver uptake; the larger the size, the faster and more extensive was the liver uptake. Both types of liposome preparations were shown to be efficient liver susceptibility agents both ex vivo and in vivo due to their uptake by the Kupffer cells of liver. The lack of full correlation between the extent of liver uptake and degree of contrast enhancement might be attributed to different regimes of susceptibility-based relaxation.

CONCLUSIONS. The present study has demonstrated the influence of key liposomal physicochemical properties on the liver uptake and contrast efficacy of liposome-encapsulated Gd chelates, exemplified by

Gd-HP-DO3A.

LIPOSOMES HAVE shown their usefulness as carriers for paramagnetic and superparamagnetic contrast materials.1-3 Because of an efficient uptake into the mononuclear phagocyte system (MPS) of liver and spleen, such liposomes have been evaluated as contrast agents for hepatosplenic imaging. Recently, the use of paramagnetic polymerized liposomes has been proposed for magnetic resonance angiography.4 Active targeting has been reported for paramagnetic liposomes labeled with antibody against integrin receptors, the latter being a marker for tumor angiogenesis.5 Most of the research on paramagnetic liposomes has centered on their efficacy as positive (T1) agents. Studies have shown a positive liver contrast effect for liposomes containing surface attached or encapsulated gadolinium (Gd) chelates.2,6,7 However, the confinement of a high concentration of paramagnetic material within Kupffer cells of the liver MPS could strongly reduce T2 through "bulk susceptibility effects" and produce a negative liver contrast enhancement. Such effects have been reported in liver for manganese (Mn) carbonate and Gd-DTPA labeled particles.8,9 The susceptibility effect arises from water molecules diffusing in the vicinity of the Kupffer cell, which acts as a large magnetic particle due to the global magnetization of the paramagnetic ions. Although the susceptibility effect is indeed a dipolar interaction, it can be distinguished from the classical inner- and outer-sphere dipolar relaxation enhancement because it does not require a close contact between water molecules and the individual paramagnetic species, but rather acts over large distances. For purposes of clarity, a distinction will be made between "susceptibility effect" and classical "dipolar relaxation" throughout the article.

As liposomes target the contrast material to Kupffer cells, it generally is mandatory that the agent withstands the acidic environment it may encounter in the subcellular lysosomal organelles after phagocytosis. Macrocyclic Gd chelates, therefore, are considered to be more suitable candidates than linear Gd chelates for such applications.10

The present study focuses on the relaxation and imaging efficacy of liposome encapsulated Gd-HP-DO3A with a special emphasis on susceptibility effects. The influence of membrane composition on the biodistribution and liver contrast efficacy of intravenously administered liposomes was investigated by ex vivo tissue relaxometry and in vivo liver imaging. An isolated and perfused rat liver model was used to assess the influence of liposome size and composition on the kinetics of liver uptake and imaging effect. Finally, the influence of size on the intrahepatic distribution of liposomes was studied.

Materials and Methods

Liposome Preparation

The following phospholipid (PL) compositions were used for liposome preparation: a blend consisting of hydrogenated phosphatidylcholine (HPC) (Lipoid GmbH, Ludwigshafen, Germany) and the sodium salt of hydrogenated phosphatidylserine (HPS) (NOF Corp., Amagasaki, Japan), and a mixture composed of dipalmitoylphosphatidylcholine (DPPC) and the sodium salt of dipalmitoylphosphatidylglycerol (DPPG) (Sygena Ltd., Liestal, Switzerland). The PL mixtures contained 5% (w/w) of the negatively charged HPS and DPPG. Thin films of PLs were hydrated in 250 mM isotonic solutions of Gd-HP-DO3A (diluted ProHance, Bracco Spa, Milano, Italy) to form multilamellar vesicles. The total PL concentration was 50 mg/mL. After a swelling period of 2 hours, the vesicles were freeze-thawed three times in liquid nitrogen and sized down by membrane extrusion (Lipex Extruder, Lipex Biomembranes Inc., Vancouver, Canada). The PL hydration, swelling and extrusion procedures were performed at temperatures of 55[degrees] and 70[degrees]C, temperatures well above the gel-to-liquid phase transition temperature (T_m) of the PLs (see Physicochemical Characterization for T_m values of the PL blends). Untrapped Gd-HP-DO3A was removed by dialysis (Spectra/Por membrane tubing MW cutoff 10000 D, Spectrum, Houston, TX) against isotonic glucose 5% (w/v) (glucose 50 mg/mL, B. Braun AG, Melsungen, Germany). The effective Gd concentration of the liposome formulations, defined as the Gd concentration in the total sample volume, was determined by inductively coupled plasma atomic emission spectrophotometry (ICP-AES), as by Fossheim et al.11

Physicochemical Characterization

The resulting liposomes, obtained after sequential membrane extrusion, were assumed to be highly unilamellar, based on previously reported ^{31}P nuclear magnetic resonance spectroscopy studies.12,13 The physicochemical properties of the liposome preparations are given in Table 1. The osmolality, measured by vapor phase osmometry, ranged from 288 to 320 mosmol/kg water (Wescor Vapor Pressure Osmometer 5500 XR, Wescor Inc., Logan, UT). The mean intensity-weighted hydrodynamic diameter of the liposome formulations ranged from 74 to 304 nm, as determined by photon correlation spectroscopy at a scattering angle of 90[degrees] and 25[degrees]C (BI-9000AT/BI-160/BI60, Brookhaven Instruments Corp., Holtsville, NY and ZetaSizer IV, Malvern Instruments Ltd., Malvern, UK). The polydispersity index, an indicator of the width of liposome size distribution, varied from 0.10 to 0.23. The mean electrophoretic mobility and zeta potential values ranged from -1.1 to -3.5 [mu]m cm/V s and from -16.1 to -50.3 mV, respectively, as determined by laser Doppler velocimetry at 25[degrees]C (ZetaPlus, Brookhaven Instruments Corp., Holtsville, NY and ZetaSizer IV, Malvern Instruments Ltd., Malvern, UK). The mean gel-to-liquid crystalline phase transition temperature (T_m) of some selected HPC/HPS and DPPC/DPPC preparations was 50.8 +/- 1.0[degrees]C and 41.4 +/- 0.5[degrees]C, respectively, as measured by differential scanning calorimetry (DSC 7, Perkin Elmer Inc., Norwalk, CT). T_m is the temperature at which the PLs undergo a conformational change and the PL bilayer converts from a gel-like to a fluid state, concomitant with a marked increase in membrane permeability toward solutes and water.14 T_m was assumed to be size independent in the studied liposome size range.15 The effective Gd concentration of the liposome preparations varied from 8.3 to 31.0 mM Gd. At 37[degrees]C and 0.47 T, the relaxivities of 250 mM Gd-HP-DO3A encapsulated into HPC/HPS and DPPC/DPPG liposomes, were shown to be exchange limited and substantially lower than those of nonliposomal metal chelate.11

Liposome composition	Liposome diameter (nm)*†	Electrophoretic mobility† (μm cm/V s)	Zeta potential† (mV)	Osmolality (mosmol/kg)	Animal experiment
DPPC/DPPG	169 ± 2	−3.5	−50.3	300	In vivo liver imaging
	163 ± 1	−1.1‡	−16.2‡	—	Ex vivo liver imaging, exp. 1
	74 ± 4	−1.7	−25.4	288	Ex vivo liver imaging, exp. 2
	103 ± 2	−1.8	−26.5	299	Ex vivo liver imaging, exp. 2
	304 ± 9	−1.8	−26.2	306	Ex vivo liver imaging, exp. 2
	153 ± 1	−1.7	−25.6	—	Ex vivo tissue relaxometry
HPC/HPS	136 ± 4	−2.8	−41.6	320	In vivo liver imaging
	143 ± 2	−1.1‡	−16.1‡	—	Ex vivo liver imaging, exp. 1
	170 ± 1	−1.6	−25.0	—	Ex vivo tissue relaxometry

* Intensity-weighted diameter (mean ± SEM).
† pH 7.4 and 25°C unless otherwise stated.
‡ pH 5.
DPPC: dipalmitoylphosphatidylcholine; DPPG: dipalmitoylphosphatidylglycerol; HPC: hydrogenated phosphatidylcholine; HPS: hydrogenated phosphatidylserine.

TABLE 1. Physicochemical Properties of Liposomal Gd-HP-DO3A

Ex Vivo Tissue Relaxometry

The DPPC/DPPG and HPC/HPS liposomes (Table 1) were administered intravenously to male Sprague Dawley rats (Mollegaard Breeding Centre, Ejby, Denmark) at a dosage of 150 [mu]mol Gd/kg body weight (n = 3). The injection volumes were 0.65 or 0.80 mL/100g and the injection rate was 1.0 mL/min. Glucose 5% was intravenously injected to control rats; a historical control group (n = 10) from a previous study was used for this purpose.9 The rats were anesthetized after 60 minutes by an intraperitoneal injection of pentobarbital (sodium pentobarbital 50 mg/mL; Nycomed Pharma AS, Oslo, Norway). The rats were laparotomized and blood was withdrawn from the vena cava; the latter was then severed to kill the rats. Ex vivo relaxation times of excised spleen, lungs, liver, and withdrawn blood were recorded at 37[degrees]C and 0.47 T (Minispec PC 120b, Bruker GmbH, Rheinstetten, Germany). Relaxation times of homogenized liver also were measured (Ika Werk TP 18-10 homogenizer, Ika Werk, Staufen i. Breisgau, Germany). T1 relaxation times were obtained by the inversion recovery method. T2 relaxation times were determined using a Carr Purcell Meiboom Gill spin echo (SE) pulse sequence with an echo time (TE) of 4 ms. The Gd content in blood and liver samples was determined by ICP-AES (described later).

In Vivo Liver Imaging

The DPPC/DPPG and HPC/HPS liposomes (Table 1) were injected intravenously to male Wistar (Mollegaard Breeding Center) rats at dosages of 150 and 300 [mu]mol Gd/kg body weight (*n* = 3-4). The injection volumes varied from 0.5 to 1.2 mL/100g and the injection rate was 1.0 mL/min. The rats first were anesthetized by subcutaneous administration of a 1:1 mixture of fentanyl/fluanison (Hypnorm, Janssen, Beerse, Belgium) and midazolam (Dormicum, F. Hofmann-La Roche AG, Basel, Switzerland), followed by intravenous injection of a 1:5 diluted fentanyl/fluanison solution approximately every 40 minutes. For comparative purposes, Gd-HP-DO3A was given intravenously to rats at a dosage of 300 [mu]mol Gd/kg body weight (*n* = 3). Gradient recalled echo (GRE), T2-weighted turbo SE and T1-weighted SE axial liver images were obtained at 2.4 T prior to and 30 and 60 minutes after liposome administration (Biospec 24/30, Bruker GmbH, Ettlingen, Germany). The following pulse sequence parameters were used: T1-weighted SE: repetition time [TR]/echo time [TE] = 113/13 ms; T2-weighted SE: TR/TE = 2112/60 ms; GRE; TR/TE/flip angle = 80/6 ms/20[degrees]. A GRE sequence with a 9 ms TE was used for the HPC/HPS liposomes at the highest dosage. For all imaging experiments, the following parameters were fixed: field of view, 7 x 7 cm; matrix size, 128 x 128; number of slices, 3; slice thickness, 4 mm. The central slice was selected for image analysis. The mean signal intensity of the liver (SI_{liver}) was measured within a freehand-drawn region of interest (ROI) in the liver parenchyma. In the background noise, the mean signal intensity (SI_{noise}) was measured within a large rectangular ROI, located in an area not affected by motion artifacts. The relative contrast enhancement (RCE) in liver parenchyma was calculated as: RCE = 100 x (SNR_{post} - SNR_{pre})/SNR_{pre}, where SNR_{post} and SNR_{pre} are the signal-to-noise ratios, SI_{liver}/SI_{noise}, of liver after and before liposome administration. The rats went into surgical anesthesia by intraperitoneal injection of sodium pentobarbital (sodium pentobarbital 60 mg/mL, Apoteks-bolaget, Umea, Sweden). Blood was withdrawn by cardiac puncture followed by excision of the liver, spleen, lungs, and kidneys. ICP-AES analysis was performed on tissue and blood samples (as described later).

Ex Vivo Liver Imaging

The contrast efficacy of liposomes of different PL composition and size (experiments 1 and 2, Table 1) was assessed in an isolated and perfused liver model at 4.7 T (MSL 200-15, Bruker GmbH, Rheinstetten, Germany). Briefly, livers were isolated from anesthetized male Wistar rats (Iffa Credo, Brussels, Belgium) and perfused at 37[degrees]C at a constant flow (3-4 mL/min/ per g of liver) through the portal vein with 200 mL of a recirculating Krebs-Henseleit (KH) buffer saturated with carbogen (95% O_2, 5% CO_2) and supplemented with 5% (v/v) rat blood from the liver donor to mimic in vivo opsonization conditions.16 The liposomes were added to the perfusion fluid at a dosage of 150 [mu]mol Gd/kg body weight (*n* = 3). The injection volume varied from 0.45 to 1.8 mL/100g. The livers were perfused in the recirculatory mode during the 20 minutes control period and the first 70 minutes after liposome administration. For the last 30 minutes, livers were perfused in the nonrecirculatory mode by continuous addition of KH buffer. Image acquisition and sampling of perfusate (1 mL) were performed every 10 minutes, the latter only during the recirculatory period. The following T2-weighted SE imaging parameters were used: TR/TE = 1737/18 or 1702/34 ms; field of view, 4 x 4 cm; matrix size, 128 x 128; number of slices, 3; slice thickness, 3 mm. For the comparison of differently sized DPPC/DPPG liposomes (experiment 2, Table 1) a TE of 18 ms was used, whereas a longer TE of 34 ms was used in the comparative study of liposomes with different PL composition (experiment 1, Table 1). Image analysis was based on SI measurements of liver parenchyma, external reference, and background noise. The external reference was a nuclear magnetic resonance tube containing superparamagnetic iron oxides or Gd-HP-DO3A. One fixed slice was selected for SI analysis throughout the image series. Three circular ROIs were selected in liver parenchyma and two ROIs were selected in the background noise. The ROI size and localization were unaltered throughout the image analysis. For each image, the SI_{liver} and SI_{noise} values were taken as the mean intensity of the ROIs. Signal-to-reference ratios, SI_{liver}/SI_{ref} (SRR), and SNR values were calculated for test and control images. The RCE in liver was calculated for each image, as previously described, using a mean value for SRR_{pre} or SNR_{pre} (mean of two control images). Due to artifacts in the center of the image where the external reference was placed, SNR values were used to calculate the liver RCE for the comparative study of PL composition. In the study of liposome size, the liver RCE was based on SRR values.

The half-life ($t_{1/2}$) of clearance from the perfusate, determined from the Gd concentration in the perfusate, was calculated assuming first order kinetics:17,18 (Equations 1 and 2) where C is the Gd concentration in the perfusate at various time points (t) after liposome addition, C_0 is the calculated initial Gd concentration and k is the rate constant of clearance from the perfusate, obtained by regression analysis of ln C versus time curve. The clearance rate indirectly measures the rate of liver uptake mainly due to the uptake into liver cells and, possibly, to accumulation within the interstitial space of liver.

$$\ln C = \ln C_0 - kt$$

Equation 1

$$t_{1/2} = \ln 2/k$$

Equation 2

The effect of liposome size on the hepatic cellular distribution was studied by separation of parenchymal (P) cells and nonparenchymal (NP) cells (one liver per size).19 During the nonrecirculatory period, livers were perfused at high flow rate (5-7 mL/min per g of liver) with calcium free KH buffer to weaken intercellular junctions. The livers were then perfused in the recirculatory mode with KH buffer, containing 45 mg collagenase (Type IV C5138, Sigma Chemical Co., St Louis, MO) /100 mL, until fissures appeared on the Glisson capsule. The intercellular matrix of liver tissue was degraded by the action of collagenase. The capsule was ruptured with scissors and the cells were dispersed by manual agitation. The cell suspension was filtered through a double layer of gauze into centrifuge tubes. A pellet of parenchymal cells (hepatocytes) was obtained by a two-step differential centrifugation at 3200 rpm and 4[degrees]C for 5 minutes, the nonparenchymal cell fraction (Kupffer and endothelial cells) remaining in the supernatant.16 ICP-AES analysis was performed on liver and cell extract samples, as described later. All animal experiments fulfill the recommendations of the Ethical Committees of our institutions.

Elemental Tissue Analysis (ICP-AES)

The tissues and cell extracts were digested with concentrated nitric acid and 30% (v/v) hydrogen peroxide at temperatures up to 130[degrees]C.9 A known volume of a 1000 ppm scandium solution (Teknolab AS, Drobak, Norway) was added to the samples to perform a Myer-Tracy signal compensation and internal standardization. Scandium was added to the perfusate and blood samples, which were diluted with 0.1 M hydrochloric acid. The Gd concentration in the samples was determined using a multipoint standard calibration curve (Perkin Elmer Plasma 2000 ICP-AES, Perkin Elmer Inc., Norwalk, CT). Both the Gd contents per g of wet and dry tissues were determined. The tissue uptake, expressed as the percentage of the administered dose, was calculated.

Statistical Analysis

The data are given as mean values +/- standard error of the mean (SEM). One way analysis of variance was used to test for statistical differences. Probability (*P*) values were corrected for multiple comparisons by the Bonferroni method 20; $P < 0.05$ was considered statistically significant.

Results

Ex Vivo Tissue Relaxometry

The effect of DPPC/DPPG and HPC/HPS liposomes on relaxation times of tissues and blood is summarized in Table 2. Both preparations were equally efficient in reducing the liver T1, while the most marked T2 effect was observed with the HPC/HPS liposomes (HPC/HPS versus DPPC/DPPG; $P = 0.025$). Homogenization of the liver further reduced the T1, most pronouncedly for the HPC/HPS liposomes (HPC/HPS versus DPPC/DPPG; $P = 0.036$). The relaxation effect of DPPC/DPPC liposomes was the strongest in blood and spleen (HPC/HPS versus DPPC/DPPG; blood, $P = 0.003$ - spleen, $P = 0.036$). A slight T1 and T2 shortening was observed in lungs for both compositions. The Gd content in liver was higher for the HPC/HPS liposomes, consistent with a lower blood concentration, compared with the DPPC/DPPG liposomes. The blood concentration, liver content, and uptake 60 minutes after injection of HPC/HPS liposomes, were 0.210 +/- 0.002 [mu]mol Gd/mL blood, 2.54 +/- 0.13 [mu]mol Gd/g wet liver and 70.4 +/- 5.9%, respectively. The corresponding values for the DPPC/DPPG liposomes were 1.046 +/- 0.074 [mu]mol Gd/mL blood, 1.93 +/- 0.27 [mu]mol Gd/g wet liver and 45.6 +/- 7.3%.

Liposome composition	T1, **T2** Relaxation times (ms)				
	Liver	Liver, homog.	Spleen	Lungs	Blood
DPPC/DPPG	231 ± 5	142 ± 3	128 ± 6	487 ± 17	588 ± 45
153 nm	**31 ± 1**	**29 ± 2**	**30 ± 1**	**50 ± 1**	**128 ± 4**
HPC/HPS	229 ± 7	127 ± 2	218 ± 6	567 ± 18	897 ± 17
170 nm	**28 ± 1**	**30 ± 1**	**29 ± 1**	**62 ± 3**	**189 ± 4**
Control*	295 ± 4	289 ± 1	573 ± 16	649 ± 13	1036 ± 17
	49 ± 1	**48 ± 1**	**65 ± 2**	**72 ± 2**	**316 ± 3**

* Glucose 5% solution; results taken from Ref. 9.
Data are given as mean ± SEM (control: $n = 10$, test dosage: $n = 3$); **bold** indicates T2 relaxation times.
DPPC: dipalmitoylphosphatidylcholine; DPPG: dipalmitoylphosphatidylglycerol; HPC: hydrogenated phosphatidylcholine; HPS: hydrogenated phosphatidylserine.

TABLE 2. Ex Vivo Tissue and Blood Relaxation Times 60 Minutes After Intravenous Administration of Liposomal Gd-HP-DO3A to Rats at a Dosage of 150 [mu]mol Gd/kg (37[degrees]C, 0.47 T)

In Vivo Liver Imaging

On GRE, T2-weighted and T1-weighted SE images, a time-persistent negative RCE in liver was obtained for both DPPC/DPPG and HPC/HPS liposomes (Table 3). Nonliposomal Gd-HP-DO3A did not produce any liver contrast enhancement. No significant difference in RCE was observed for the preparations on the T1-weighted and T2-weighted SE images. Only on GRE images at the highest dosage, were the HPC/HPS liposomes the most efficient contrast enhancers (HPC/HPS versus DPPC/DPPG; $P < 0.020$ at both time points) (Fig. 1). The RCE was dose-dependent only for the HPC/HPS liposomes on the GRE images (150 versus 300 [mu]mol/kg; $P < 0.043$ at both time points), and a longer TE increased the negative RCE from -61 +/- 2 to -76 +/- 2% and from -63 +/- 1 to -77 +/- 1% at 30 and 60 minutes, respectively. The Gd content in tissues and blood is given in Table 4. The liver Gd content and uptake were slightly higher but not statistically different for the HPC/HPS liposomes. The apparent discrepancies between these liver uptake results and those from the ex vivo tissue relaxometry will be discussed later. No significant retention of liposomes was detected in lungs. A higher concentration of Gd in blood was obtained for the DPPC/DPPG liposomes at the highest dosage (HPC/HPS versus DPPC/DPPG; $P = 0.001$). The Gd content in tissues and blood was low after the administration of nonliposomal Gd-HP-DO3A, the highest Gd deposition being found in the kidneys. A similar tissue distribution profile has been reported in mice after an intravenous injection of Gd-HP-DO3A at a dosage of 480[mu]mol Gd/kg.21

Liposome composition	Dosage (μmol Gd/kg)	% Relative liver contrast enhancement					
		T1-w SE		T2-w SE		GRE	
		30 min	60 min	30 min	60 min	30 min	60 min
DPPC/DPPG	150	−27 (±2)	−31 (±7)	−51 (±1)	−56 (±3)	−38 (±8)	−39 (±9)
169 nm	300	−26 (±2)	−24 (±8)	−69 (±3)	−56 (±7)	−44 (±3)	−44 (±5)
HPC/HPS	150	−28 (±2)	−28 (±2)	−55 (±2)	−60 (±4)	−45 (±6)	−44 (±3)
136 nm	300	−37 (±2)	−32 (±3)	−65 (±1)	−64 (±3)	−61 (±2)	−63 (±1)
Control*	300	+11 (±6)	+1 (±4)	−9 (±16)	−13 (±16)	+2 (±2)	−2 (±3)

* Nonliposomal Gd-HP-DO3A. Data are given as mean ± SEM ($n = 3$–4).
T1-w SE – TR/TE = 113/13 ms; T2-w SE – TR/TE = 2112/60 ms; GRE – TR/TE/flip angle = 80/6 ms/20°.
SE: spin echo, GRE: gradient recalled echo; DPPC: dipalmitoylphosphatidylcholine; DPPG: dipalmitoylphosphatidylglycerol; HPC: hydrogenated phosphatidylcholine; HPS: hydrogenated phosphatidylserine.

TABLE 3. In Vivo Liver Contrast Enhancement After Intravenous Administration of Liposomal Gd-HP-DO3A to Rats (2.4 T)

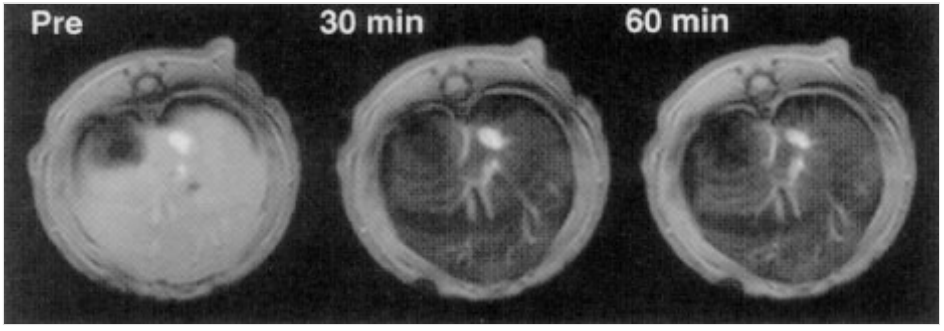

Figure 1. Gradient recalled echo axial images of rat liver prior to, 30 and 60 minutes after intravenous administration of HPC/HPS-based Gd-HP-DO3A liposomes at a 300 [mu]mol Gd/kg dosage (2.4 T).

Liposome composition	Dosage (μmol Gd/kg)	Tissue and Blood Content (μmol Gd/g wet tissue or mL blood) **Percent of Administered Dosage in Tissue and Blood***				
		Liver	Spleen	Lungs	Kidneys	Blood
DPPC/DPPG	150	0.895 ± 0.129 **29.9 ± 4.5**	5.500 ± 0.379 **17.9 ± 2.1**	0.566 ± 0.100 **2.6 ± 0.5**	0.889 ± 0.183 **5.7 ± 1.1**	0.107 ± 0.011 **3.8 ± 0.4**
169 nm	300	1.388 ± 0.285 **23.4 ± 4.5**	10.59 ± 1.48 **15.4 ± 1.5**	0.361 ± 0.04 **1.1 ± 0.2**	1.006 ± 0.390 **4.1 ± 2.2**	0.660 ± 0.03 **12.1 ± 0.7**
HPC/HPS	150	0.873 ± 0.080 **29.2 ± 2.1**	11.45 ± 0.77 **37.9 ± 4.0**	0.215 ± 0.053 **1.2 ± 0.3**	0.155 ± 0.024 **1.4 ± 0.3**	0.090 ± 0.012 **3.3 ± 0.4**
136 nm	300	1.603 ± 0.126 **28.0 ± 0.6**	16.93 ± 2.24 **28.9 ± 3.6**	0.339 ± 0.042 **0.8 ± 0.1**	0.223 ± 0.014 **1.0 ± 0.2**	0.302 ± 0.041 **5.5 ± 0.7**
Control†	300	0.057 ± 0.003 **1.0 ± 0.1**	0.06 ± 0.012 **0.08 ± 0.01**	0.198 ± 0.039 **0.4 ± 0.1**	1.640 ± 0.563 **4.2 ± 1.5**	0.095 ± 0.032 **1.47 ± 0.78**

* Assuming that the blood volume represents 5.4% (v/w) of the body weight.[31]
† Nonliposomal Gd-HP-DO3A.
Data are given as mean ± SEM (n = 3–4). For purposes of clarity, the metal content/g of dry tissue is not reported. **Bold** indicates uptake.
HPC: hydrogenated phosphatidylcholine; HPS: hydrogenated phosphatidylserine; DPPC: dipalmitoylphosphatidylcholine; DPPG: dipalmitoylphosphatidylglycerol.

TABLE 4. Tissue and Blood Deposition of Gd 60 Minutes After Intravenous Administration of Liposomal Gd-HP-DO3A to Rats (In Vivo Imaging Experiments at 2.4 T)

Ex Vivo Liver Imaging

Experiment 1. Figure 2A summarizes the influence of membrane composition on the uptake kinetics of liposomal Gd-HP-DO3A in the perfused rat liver. The liver uptake was extensive and rapid for the HPC/HPS liposomes and was essentially completed after 40 minutes. The uptake kinetics were slower for the DPPC/DPPG liposomes, the liver still taking up liposomes at the end of the recirculatory perfusion. The half-life of elimination from the perfusate was 24 +/- 2 and 63 +/- 7 minutes for the HPC/HPS and DPPC/DPPG preparations, respectively. For the HPC/HPS liposomes, the liver content was 1.750 +/- 0.063 [mu]mol Gd/g wet liver equivalent to a final uptake of 60.2 +/- 3.6%. The corresponding values for the DPPC/DPPG liposomes were 1.543 +/- 0.018 [mu]mol Gd/g wet liver and 49.9 +/- 2.4%. These uptake values were in agreement with the apparent liver uptake calculated indirectly from the Gd loss in the perfusate at the end of the recirculatory perfusion. Both liposome compositions efficiently decreased the liver SI, an effect that persisted during the nonrecirculatory perfusion period (Fig. 2B). The negative RCE was most marked for the HPC/HPS liposomes in the first part of the perfusion (P = 0.031 and 0.028 at 20 and 30 minutes, respectively), and the RCE reached its maximum at 30 minutes, approximately at the time when the liver uptake was essentially terminated. From approximately 40 minutes of perfusion, both liposome formulations were equally efficient in reducing the liver SI.

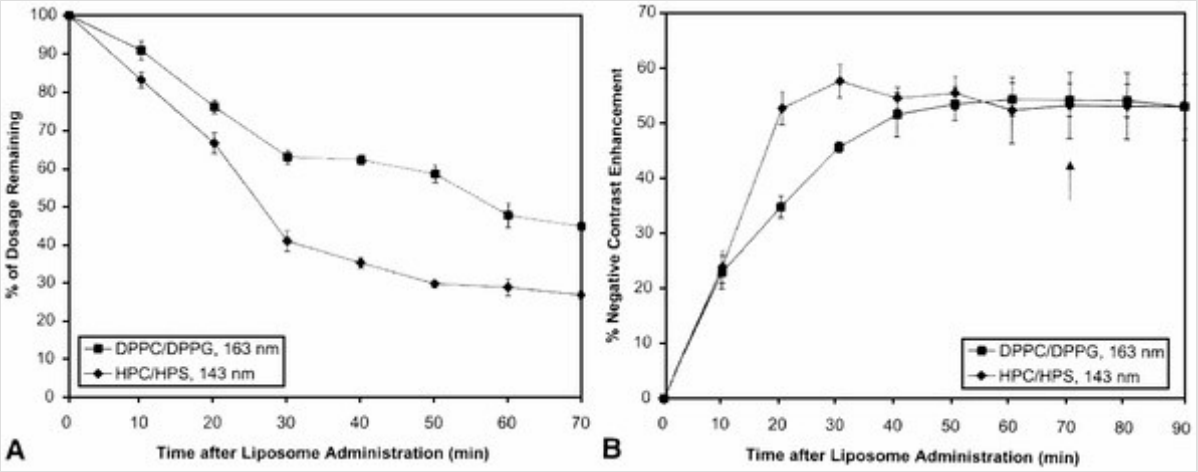

Figure 2. The influence of liposome composition on the kinetics of (A) uptake and (B) relative contrast enhancement in the perfused rat liver for liposomal Gd-HP-DO3A at a 150 [mu]mol Gd/kg dosage (37[degrees]C, 4.7 T). The start of nonrecirculatory perfusion is indicated by an arrow. Data are given as mean +/- SEM (n = 3).

Experiment 2. Figure 3A and Table 5 summarize the influence of liposome size on the liver uptake kinetics and intrahepatic distribution of DPPC/DPPG liposomes. The larger the liposome size, the more rapid and extensive was the liver uptake. Here also, the final uptake values agreed well with the apparent liver uptake calculated indirectly from the Gd loss. The half-life values were 18 +/- 2, 45 +/- 7, and 170 +/- 13 minutes for the 304, 103, and 74 nm liposomes, respectively. An intrahepatic shift of the cell type involved in liposome clearance was observed, the value of the P/NP Gd ratio (ratio of the Gd content in parenchymal versus nonparenchymal cell fractions) decreasing from 4.8 to 3.4 x 10^{-3} in the liposome size range of 74 to 304 nm. The liposome formulations gave a time-persistent negative RCE throughout the perfusion (Fig. 3B). During the nonrecirculatory liver perfusion with calcium free KH buffer (one liver per size) a reduction of approximately 50% in the RCE was observed, irrespective of liposome size. This observation might be explained by a loss of cells into the perfusate; however, this does not affect the conclusions of the present work. The RCE in the nonrecirculatory period was therefore calculated for two rats only. The smallest liposomes were the least efficient contrast enhancers throughout the perfusion (74 nm versus 103 nm; $P < 0.03$ at all time points) (Fig. 3B and Fig. 4). The 304 nm liposomes showed the most marked effect in the first 20 minutes, but during the late phase of the perfusion they were equally efficient as the intermediate 103 nm liposomes.

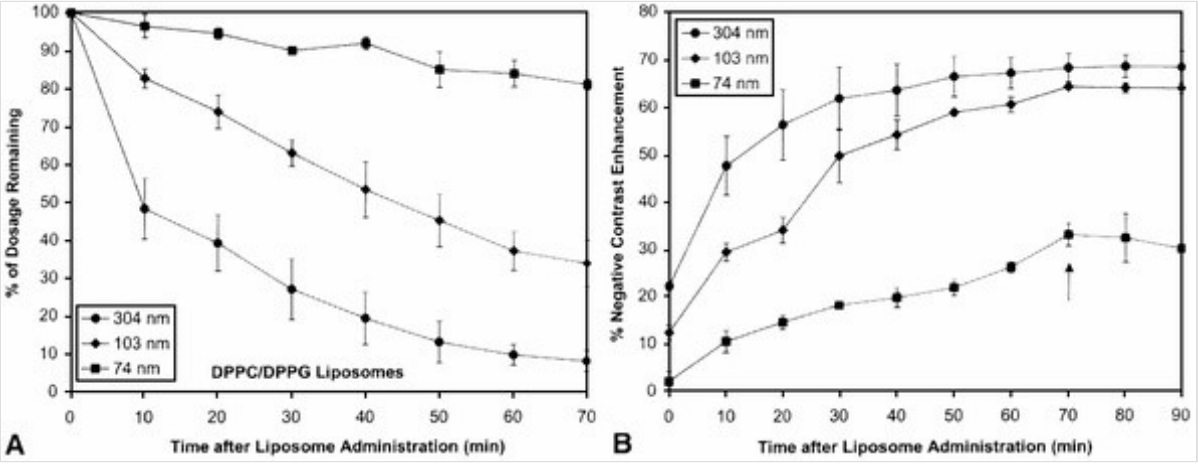

Figure 3. The influence of size on the kinetics of (A) uptake and (B) relative contrast enhancement in the perfused rat liver for DPPC/DPPG-based Gd-HP-DO3A liposomes at a 150 [mu]mol Gd/kg dosage (37[degrees]C, 4.7 T). The start of nonrecirculatory perfusion is indicated by an arrow. Data are given as mean +/- SEM (n = 2-3).

Liposome size	Liver content (μmol Gd/g wet liver) **Liver uptake (Percent of administered dosage)**	P/NP Gd ratio*
74 nm	0.331 ± 0.019 **13.0 ± 2,4**	4.8
103 nm	1.659 ± 0.157 **56.7 ± 5.6**	0.20
304 nm	2.767 ± 0.290 **83.9 ± 6.7**	3.4×10^{-3}

* n = 1. Data are given as mean ± SEM (n = 2). **Bold** indicates liver uptake.

For purposes of clarity, the metal content/g of dry tissue is not reported.

P/NP Gd ratio: ratio of the Gd content in parenchymal vs non-parenchymal cell fractions.

TABLE 5. Liver Deposition and Microdistribution of Gd in the Perfused Rat Liver After Administration of DPPC/DPPG-Based Gd-HP-DO3A Liposomes at a Dosage of 150 [mu]mol Gd/kg

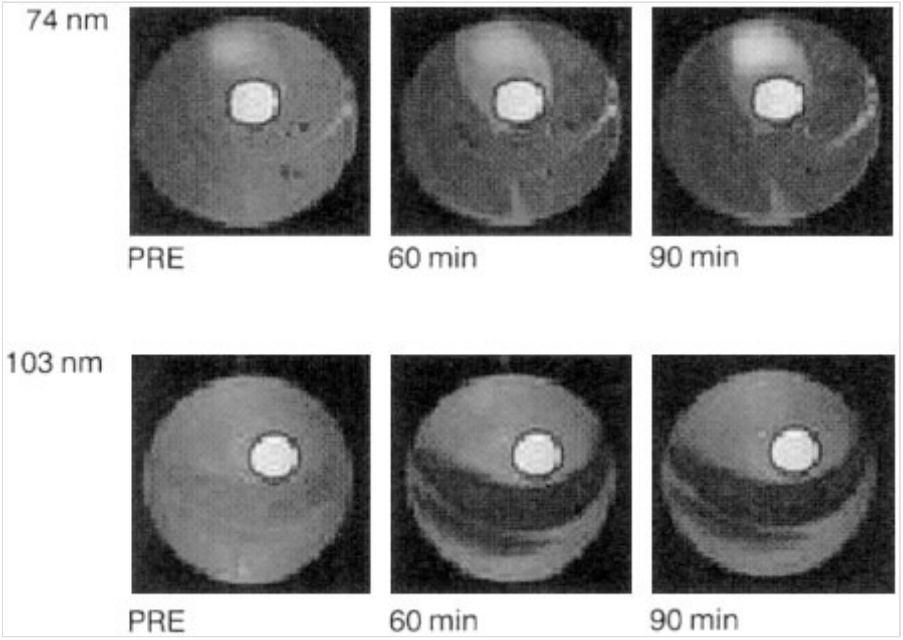

Figure 4. T2-weighted spin echo axial images of the perfused rat liver before and 30 and 90 minutes after administration of differently sized DPPC/DPPG-based Gd-HP-DO3A liposomes at a 150 [mu]mol Gd/kg dosage (37[degrees]C, 4.7 T). (Note the central position of the external reference).

Discussion

As are all foreign surfaces, intravascularly administered liposomes are opsonized and cleared from blood through phagocytosis by the MPS in liver and spleen. Numerous studies have shown that the opsonization process and, hence, the liver uptake are influenced by physicochemical factors such as the PL composition, size and surface charge of the liposome.22 In addition, depending on size, uptake into hepatocytes may occur.22 There is no consensus on the critical size of liposomes for passive targeting to the hepatocytes. The endothelial fenestrations in the liver sinusoids have an average diameter of approximately 100 nm,23 and it has been postulated that liposomes smaller than 100 nm should access the hepatocytes.

Ex Vivo Tissue Relaxometry

In these experiments, the influence of membrane composition on the liver uptake could be assessed directly because both investigated vesicle preparations displayed similar surface charge and size (Table 1). Due to the relatively large size of both preparations, a possible uptake by the hepatocytes could be discarded, and the liposomes were assumed to be taken up by the Kupffer cells of the liver MPS. The higher liver uptake of the HPC/HPS liposomes, compared with the DPPC/DPPG ones, was attributed both to the HPS component and to the higher liposome stability in blood. The improved stability of the HPC/HPS liposomes was attributed to the substantially higher T_m relative to physiologic temperature. Features such as a low membrane permeability 11 and a reduced risk of bilayer destabilization or disintegration (processes mainly mediated by blood components), minimize the liposome leakage of metal chelate in the bloodstream.22 Studies have evidenced that the presence of PS on the liposome surface promotes also a direct opsonization-independent liver uptake in rats and the existence of a specific PS receptor on MPS macrophages has been postulated.24 Because PS and HPS have the same head group structure, the affinity of the PS receptor toward HPS should not be different.

Upon internalization into the Kupffer cells, Gd-HP-DO3A encounters an intracellular environment that is not optimal for the liposome integrity. It is reasonable to assume that Gd-HP-DO3A will exist both as free and liposomal chelate within the Kupffer cell. Encapsulated or not, intracellularly located Gd-HP-DO3A should have little influence on the T1 relaxation effect in liver. The small Kupffer cell volume (2% of the liver parenchyma),25 the slow water exchange between the interior and exterior of the cell, and the large distance between neighboring Kupffer cells 26 are factors that restrict the dipolar T1 (and T2) relaxation effect. Such limitations of the dipolar T1 contribution usually have been confirmed by liver homogenization where a markedly reduced T1 is obtained due to a release of contrast material from the Kupffer cells.27 In the present study, homogenization did not shorten the liver T1 to values predicted from the actual Gd concentrations in the tissue. These apparent discrepancies could be explained by an incomplete destruction of the Kupffer cells, but more likely of the liposomes.

The liver T1 was, however, significantly reduced despite the above mentioned limitations of the dipolar relaxation. An important contribution to the observed T1 (and T2) shortening in liver and other tissues was the dipolar relaxation effect from paramagnetic material, liposome associated or not, circulating in blood. Due to the significant T1 reduction in blood, this dipolar effect existed in liver for the DPPC/DPPG vesicles. Another contribution to the liver T1 effect could be the time-dependent extravasation of liposome-released Gd-HP-DO3A into the liver interstitium. The DPPC/DPPG vesicles were more prone to degradation in blood and, with time, released metal chelate that leaked out into liver tissue. This may explain the equivalent T1 effect in liver for both liposome compositions, despite of their different liver uptake.

More efficient T1 relaxation would be expected to occur only after intrahepatic redistribution from the small Kupffer cell compartment to larger cellular compartments, such as the hepatocytes which account for 78% of the liver parenchyma.25 Such an intrahepatic translocation has been reported for Mn chloride encapsulated within DPPC/DPPG liposomes where a marked positive contrast effect was observed only 1 hour after administration.28 Within the Kupffer cell, Mn was reported to bind to intracellular proteins immediately after release from the liposome.26,28 Manganese efflux from the Kupffer cells with subsequent uptake into the hepatocytes was explained by a facilitated diffusion process,26 although other mechanisms such as receptor mediated exocytosis/endocytosis of protein-bound Mn or diffusion of free Mn through calcium channels are plausible processes (Grant D, Hustvedt SO, personal communication, 1998). In a recent liver imaging study with Mn carbonate particles, the shift from an initial negative contrast effect to a positive liver enhancement also suggested a redistribution of Mn from Kupffer cells to the hepatocytes.8 For hydrophilic and stable metal chelates such as Gd-HP-DO3A, no dechelation nor intracellular protein binding are expected to occur.10,29 Therefore, no intrahepatic redistribution of Gd-HP-DO3A was anticipated within the time frame of the experiments.

The liver T2 shortening was due to both the susceptibility effects and, to the dipolar relaxation caused by the presence of paramagnetic material in blood and liver interstitium. For the HPC/HPS liposomes, the higher Gd concentration in Kupffer cells increased the magnitude of the susceptibility effects, which resulted in a more efficient T2 shortening compared with the DPPC/DPPG liposomes. Liver homogenization eliminated the susceptibility effects, thus causing the liver T2 to increase, but also removed the dipolar T2 relaxation limitations, and therefore counteracted the liver T2 increase. Hence, these two opposing contributions may explain the observed unchanged liver T2 after homogenization.

In Vivo Liver Imaging

The experiments were performed at a higher field strength (2.4 T), a feature that increases the magnitude of the susceptibility effects. This was evidenced by the significant decrease in liver SI on T2-weighted SE and GRE images after administration of DPPC/DPPG and HPC/HPS liposomes. There was no statistically significant difference in liver uptake between the two liposome compositions, which was reflected by a similar imaging effect at the lowest dosage. The HPC/HPS liposomes were only the most efficient negative contrast enhancers on GRE images at the highest dosage. Because different vesicle preparations were used for the tissue relaxometry and liver imaging experiments, comparisons with regard to contrast efficacy and liver uptake should be undertaken with caution (Table 1). Nevertheless, based on the tissue relaxation results, a more extensive liver uptake was expected for the HPC/HPS liposomes compared with the DPPC/DPPG ones in the current imaging study. The lack of such a finding might be explained by the dissimilar physicochemical properties of both preparations, which may have obscured the direct influence of membrane composition on liver uptake. The DPPC/DPPG liposomes displayed a slightly more negative surface charge and a larger size (Table 1), factors that are known to promote liver uptake.22 The extensive spleen deposition of the HPC/HPS liposomes also might explain the lower than anticipated liver uptake. Such a preferential spleen uptake has been reported previously for PS-containing vesicles and was attributed to the PS component.30,31 On the T1-weighted SE images, a negative RCE was observed for both liposome compositions. A positive contrast effect might have been anticipated at the highest dosage due to the presence of paramagnetic species in blood. However, the susceptibility effects were important and masked any positive liver enhancement. For comparative purposes, the imaging efficacy of nonliposomal Gd-HP-DO3A also was investigated. Due to the rapid extravascular distribution and renal elimination of the metal chelate, liver and blood concentrations were too low to observe any significant effect on the liver SI.

There have been numerous reports on the in vivo liver contrast efficacy of egg PC/cholesterol-based vesicles containing Gd-DTPA.7,32 Regardless of vesicle size or dosage, a significant positive liver contrast effect was reported at 1.5 T on T1-weighted SE images. Despite weaker susceptibility effects due to the lower field strength, the use of a fourfold longer TR was likely to produce less T1 contrast compared with the present study. The different enhancement could therefore be explained by the use of different PLs. Although cholesterol is known to improve the stability of liposomes in blood,33 PC/cholesterol-based liposomes have been reported to be more labile than the currently investigated liposomes,26 due to the substantially lower T_m of egg PC (-15 to -4[degrees]C)34 and the higher membrane permeability 26. In the previously reported studies, the positive liver effect of liposomal Gd-DTPA was attributed mainly to vesicles taken up by the liver, although a blood pool effect also was proposed as a possible explanation.7,32 Considering the limited dipolar relaxation in liver, it is rather believed that the vascular enhancement caused by a high blood concentration of paramagnetic chelate (liposomal or not) and liver extravasation of chelate were the main contributors to the positive contrast liver effect of liposomal Gd-DTPA.

Ex Vivo Liver Imaging

The ex vivo perfused rat liver has proved to be a suitable model to investigate the influence of liposomal physicochemical properties on the uptake kinetics.31 The effect of membrane composition on the hepatic uptake was assessed by the comparison of DPPC/DPPG and HPC/HPS vesicles having otherwise a similar size and surface charge (experiment 1, Table 1). For the investigation of liposome size on the liver uptake behavior, differently sized DPPC/DPPG liposomes, displaying similar surface charge, were compared (experiment 2, Table 1).

The apparently faster and higher liver uptake of the HPC/HPS liposomes, compared with the DPPC/DPPG liposomes, could be attributed to their higher stability in the perfusate and to the HPS component. The faster and more extensive liver uptake of 304 nm DPPC/DPPG liposomes compared with smaller ones was explained by an increased efficiency of the opsonization process.22 The 100 nm threshold for hepatocyte targeting also was confirmed as the 304 nm liposomes showed massive accumulation in Kupffer cells with minimal uptake into the hepatocytes, as evidenced semiquantitatively by the low P/NP Gd ratio (liposomes have shown, regardless of size, no uptake into NP endothelial cells).35 Some uptake into the hepatocytes was observed for the intermediate 103 nm liposomes, as shown by a higher value of the P/NP ratio. Finally, the 74 nm liposomes demonstrated an absolute low liver uptake but a preferential localization into the hepatocytes. These findings are consistent with previous studies reporting hepatocyte targeting for 70 nm or smaller vesicles.36,37 Also, accumulation of Gd-HP-DO3A (mostly nonliposomal) within the liver interstitium was shown to be negligible as the liver uptake was not significantly altered during the washout of the extracellular space.

All liposome preparations efficiently reduced the SI of the perfused liver at 4.7 T, an effect that persisted throughout the nonrecirculatory perfusion. This confirmed that the negative RCE was caused by the susceptibility effect of intracellularly located paramagnetic material, mainly in the Kupffer cells. Whereas liposome size and composition modulated the degree and kinetics of liver uptake, the liver contrast effect was affected differently. Except for the first 20 minutes, the 103 and 304 nm DPPC/DPPG liposomes were equally efficient in reducing the liver SI despite a different liver uptake during the remainder of the perfusion. Similarly, the initially higher and more rapid liver uptake of the HPC/HPS liposomes, compared with the DPPC/DPPG ones, was reflected by the most marked negative contrast effect up to 30 minutes after liposome administration. However, during the remainder of the perfusion the imaging effect was similar for both liposome preparations despite of a different liver uptake.

Different regimes of susceptibility-based relaxation during the early and late phases of the perfusion may offer an explanation for the lack of correlation between liver uptake and imaging efficacy. In general, for a given size and volume fraction of uniformly magnetized particles, outersphere relaxation theory predicts a quadratic dependence between T2 relaxation rate and the particle magnetization, provided the conditions of motional narrowing are met.38,39 By extrapolation to liver, the magnetic particle would be the magnetized Kupffer cell. However, the criteria of an homogeneous cell distribution, a uniform magnetization, and constant size of Kupffer cells may not be fulfilled. Kupffer cells have a scattered distribution in liver, possess heterogeneous phagocytic activity,40,41 and may vary in size upon engulfment of particles, the latter depending on the nature of the phagocytosed material.42 Nevertheless, outer-sphere relaxation theory can be used to qualitatively interpret the imaging data during the different phases of the perfusion. Initially, the liver uptake for either liposome preparation was not so high as to increase the magnetization to the extent that the conditions of motional narrowing would be strongly violated. Differences in liver uptake were reflected in differences in the negative contrast effect. The higher imaging efficacy of the HPC/HPS liposomes compared with the DPPC/DPPG ones during the first 30 minutes of perfusion could be attributed to the higher uptake of Gd, magnetizing the Kupffer cells to a larger extent. Analogously, the higher uptake of the 304 nm DPPC/DPPG liposomes compared with the smaller 103 nm ones was reflected in a more marked RCE up to 20 minutes. However, as the perfusion continued, the liver uptake and, therefore, the magnetization, increased to the extent that the criterion of motional narrowing failed. During a time duration approximately equal to TE, water molecules did not diffuse very far with respect to the dimensions of the magnetic field created by the Kupffer cells. Consequently, the liver T2 was not sensitive to further increases in the magnetization of the Kupffer cells.38 Therefore, the liposome preparations should display similar imaging efficacy in liver, as observed. The supposition that the liver T2 may not always be correlated to liver concentration has previously been suggested in the case of iron oxides 43,44 and T2-weighted SE imaging studies in liver have shown a "saturation" of the negative contrast effect with increasing liver deposition of iron.45

The negative contrast effect of the 74 nm DPPC/DPPG liposomes was high considering the low liver uptake. Despite a four- to sixfold lower uptake compared with larger liposomes, the contrast efficacy was only approximately 50% lower. As the 74 nm liposomes were mostly located in the hepatocytes, the RCE observed must mainly be mediated through classical dipolar relaxation, assuming some liposome degradation occurred within the time frame of the experiments.26,28 However, the more homogeneous distribution of paramagnetic material throughout the hepatic tissue also may be a contributing factor to the nonnegligible susceptibility effects.

Conclusion

The present study has demonstrated the influence of liposomal physicochemical properties on the liver uptake and contrast efficacy of liposome encapsulated Gd chelates, exemplified by Gd-HP-DO3A. The liver uptake was shown to be modulated by the liposome size and membrane composition. HPC/HPS liposomes demonstrated generally a more extensive and faster uptake than DPPC/DPPG liposomes due to a higher liposome stability and to the HPS component. The larger the liposome size, the faster and higher was the liver uptake. Also, a gradual shift in the cell type involved in liposome clearance was observed as the liposome size decreased. The various imaging experiments have highlighted the poor correlation between the in vitro efficacy and liver contrast enhancement of paramagnetic particles, liposomal Gd-HP-DO3A being an efficient negative contrast agent despite a low in vitro T2 relaxivity.11 Susceptibility effects, caused by a high concentration of Gd-HP-DO3A confined within the Kupffer cells, were mostly responsible for the negative liver contrast enhancement. Such paramagnetic susceptibility effects in liver are independent of relaxivity and are only modulated by the magnetization of the Kupffer cells, which is given by the field strength, magnetic susceptibility and intracellular concentration of the agent. Also, the lack of complete correlation between liver uptake and negative contrast effect could be attributed to different regimes of susceptibilitybased relaxation. The various studies have shown that paramagnetic vesicles, whose stability is high enough to permit an efficient liver uptake, will only function as negative liver agents as long as the size is approximately 100 nm or above. Finally, the importance of reproducibility in liposome preparation, with regard to size and surface charge, should be mentioned. In some instances, batch-to-batch variations complicated the assessment of the influence of a given physicochemical parameter on the liver uptake. Although one may think that such problems can be avoided by the use of the same vesicle preparation for various studies, liposome stability and leakage of encapsulated chelate during long term storage may be serious limitations.

Acknowledgments

The authors thank C. Johansson, K. Thyberg (Dept. of Experimental Research, Malmo University Hospital, Malmo, Sweden), K.A. Bjerkeli, B. Spilling (Nycomed Imaging AS, Oslo, Norway) and C. Pierart (NMR Laboratory, University of Mons-Hainaut, Mons, Belgium) for providing technical assistance, and K.E. Kellar (Nycomed Amersham Imaging, Wayne, PA) for valuable discussions.

References

1. ger E, Fritz T, Wu G, et al. Liposomal MR contrast agents. J Liposome Res 1994;4:811-834. [Context Link]

2. Krause W, Klopp R, Leike J, Sachse A, Schuhmann-Giampieri G. Liposomes in diagnostic imaging: Comparison of modalities-In vivo visualization of liposomes. J Liposome Res 1995;5:1-26. Link Resolver | Bibliographic Links | [Context Link]

3. Bogdanov AA, Martin C, Weissleder R, Brady T. Trapping of dextrancoated colloids in liposomes by transient binding to aminophospholipid:preparation of ferrosomes. Biochim Biophys Acta 1994;1193:212-218. Link Resolver | Bibliographic Links | [Context Link]

4. Storrs RW, Tropper FD, Li HY, et al. Paramagnetic polymerized liposomes as new recirculating MR contrast agents. J Magn Reson Imaging 1995;5:719-724. Link Resolver | Bibliographic Links | [Context Link]

5. Sipkins DA, Kazemi M, Cheresh D, Bednarski MD, Li KCP. Detection of tumor angiogenesis in vivo by [alpha]$_V$[beta]$_3$-targeted magnetic resonance imaging. Proceedings of the Fifth Scientific Meeting of the International Society for Magnetic Resonance in Medicine 1997:334. [Context Link]

6. Kabalka GW, Davis MA, Holmberg E, Maruyama K, Huang L. Gadolinium-labeled liposomes containing amphiphilic Gd-DTPA derivatives of varying chain length:targeted MRI contrast enhancement agents for the liver. Magn Reson Imaging 1991;9:373-377. Link Resolver | Full Text | Bibliographic Links | [Context Link]

7. Unger EC, Winokur T, MacDougall P, et al. Hepatic metastases: Liposomal Gd-DTPA-enhanced MR imaging. Radiology 1989;171:81-85. Link Resolver | Bibliographic Links | [Context Link]

8. Wisner ER, Merisko-Liversidge E, Kellar K, et al. Preclinical evaluation of manganese carbonate particles for magnetic resonance imaging of the liver. Acad Radiol 1995;2:140-147. Link Resolver | Full Text | Bibliographic Links | [Context Link]

9. Fossheim SL, Kellar KE, Mansson S, et al. Investigation of lanthanide-based starch particles as a model system for liver contrast agents. J Magn Reson Imaging. In press. [Context Link]

10. Unger EC, Fritz TA, Tilcock C, New TE. Clearance of liposomal gadolinium:in vivo decomplexation. J Magn Reson Imaging 1991;1:689-693. Link Resolver | Bibliographic Links | [Context Link]

11. Fossheim SL, Fahlvik AK, Klaveness J, Muller RN. Paramagnetic liposomes as MRI contrast agents: Influence of liposomal physicochemical properties on the in vitro relaxivity. Magn Reson Imaging. In press. [Context Link]

12. Fossheim S, Vander Elst L, Muller RN. Application of ^{31}P NMR spectroscopy in liposome characterization. Scientific Program and Book of Abstracts, 13th Annual Meeting European Society for Magnetic Resonance in Medicine and Biology 1996;IV(II supp):301. [Context Link]

13. Hope MJ, Bally MB, Webb G, Cullis PR. Production of large unilamellar vesicles by a rapid extrusion procedure. Characterization of size distribution, trapped volume and ability to maintain a membrane potential. Biochim Biophys Acta 1985;812:55-65. Link Resolver | Bibliographic Links | [Context Link]

14. Mouritsen OG, Jorgensen K, Honger T. In: Disalvo EA, Simon SA, eds. Permeability and stability of lipid bilayers. Boca Raton, FL: CRC Press Inc., 1995. [Context Link]

15. Biltonen RL, Lichtenberg D. The use of differential scanning calorimetry as a tool to characterize liposome preparations. Chem Phys Lipids 1993;64:129-142. Link Resolver | Full Text | Bibliographic Links | [Context Link]

16. Colet JM. Study of the mechanisms of hepatic internalization of molecular and nanoparticular systems, contrast agents for magnetic resonance imaging. Mons, Belgium: University of Mons-Hainaut, 1995. Doctorate thesis. [Context Link]

17. Rowland M, Tozer TN. In: Clinical pharmacokinetics: Concepts and applications. Malvern, PA: Lea & Febiger, 1989. [Context Link]

18. Nicholas AR, Jones MN. The absorption of phospholipid vesicles by perfused rat liver depends on vesicle surface charge. Biochim Biophys Acta 1986;860:600-607. Link Resolver | Bibliographic Links | [Context Link]

19. Seglen PO. In: Prescott DM, ed. Methods in cell biology. Vol. 13. New York, NY: Academic Press Inc., 1976. [Context Link]

20. Altman DG. In: Practical statistics for medical research. London, England: Chapman & Hall, 1995. [Context Link]

21. Tweedle MF, Wedeking P, Kumar K. Biodistribution of radiolabeled, formulated gadopentetate, gadoteridol, gadoterate, and gadodiamide in mice and rats. Invest Radiol 1995;30:372-380. Ovid Full Text | Link Resolver | Bibliographic Links | [Context Link]

22. Harashima H, Kiwada H. Liposomal targeting and drug delivery: kinetic consideration. Adv Drug Deliv Rev 1996;19:425-444. Link Resolver | Full Text | Bibliographic Links | [Context Link]

23. Wisse E, De Zanger RB, Charels K, Van Den Smisse P, Mc Cuskey RS. The liver sieve considerations concerning the structure and function of endothelial fenestrae, the sinusoidal wall and the space of Disse. Hepatology 1985;5:683-692. Link Resolver | Full Text | Bibliographic Links | [Context Link]

24. Scherphof GL, Crommelin DJA. Cells involved in removing liposomes from the blood circulation: Why are they so special? J Liposome Res 1996;6:19-32. Link Resolver | Bibliographic Links | [Context Link]

25. Blouin A, Bolender RP, Weibel ER. Distribution of organelles and membranes between hepatocytes and nonhepatocytes in the rat liver parenchyma:a stereological study. J Cell Biol 1977;72:441-455. Link Resolver | Bibliographic Links | [Context Link]

26. Bacic G, Niesman MR, Magin RL, Swartz HM. NMR and ESR study of liposome delivery of Mn^{2+} to murine liver. Magn Reson Med 1990;13:44-61. Link Resolver | Bibliographic Links | [Context Link]

27. Fahlvik AK, Holtz E, Klaveness J. Relaxation efficacy of paramagnetic and superparamagnetic microspheres in liver and spleen. Magn Reson Imaging 1990;8:363-369. Link Resolver | Full Text | Bibliographic Links | [Context Link]

28. Magin RL, Wright SM, Niesman MR, Chan HC, Swartz HM. Liposome delivery of NMR contrast agents for improved tissue imaging. Magn Reson Med 1986;3:440-447. Link Resolver | Bibliographic Links | [Context Link]

29. Choyke PL, Girton ME, Vaughan EM, Franck JA, Austin HA III. Clearance of gadolinium chelates by hemodialysis: An in vitro study. J Magn Reson Imaging 1995;4:470-472. [Context Link]

30. Spanjer HH, Van Galen M, Roerdink FH, Regts J, Scherphof GL. Intrahepatic distribution of small unilamellar liposomes as a function of liposomal lipid composition. Biochim Biophys Acta 1986;863:224-230. Link Resolver | Bibliographic Links | [Context Link]

31. Liu D. Animal species dependent liposome clearance. J Liposome Res 1996;6:77-97. Link Resolver | Bibliographic Links | [Context Link]

32. Unger EC, Mac Dougall P, Cullis P, Tilcock C. Liposomal Gd-DTPA: Effect of encapsulation on enhancement of hepatoma model by MRI. Magn Reson Imaging 1989;7:413-423. Link Resolver | [Context Link]

33. Lasic DD. In: Liposomes from physics to applications. Amsterdam, The Netherlands: Elsevier Science Publishers BV, 1993. [Context Link]

34. Szoka F Jr, Papahadjopoulos D. Comparative properties and methods of preparation of lipid vesicles (liposomes). Ann Rev Biophys Bioeng 1980;9:467-508. [Context Link]

35. Rahman YE, Cerny EA, Patel KR, Lau EH, Wright BJ. Differential uptake of liposomes varying in size and lipid composition by parenchymal and Kupffer cells of mouse liver. Life Sci 1982;31:2061-2071. Link Resolver | Full Text | Bibliographic Links | [Context Link]

36. Vion-Dury J, Masson S, Devoisselle JM, et al. Liposome-mediated delivery of gadolinium-diethylenetriaminopentaacetic acid to hepatic cells: A P-31 NMR study. J Pharmacol Exp Ther 1989;250:1113-1118. Link Resolver | Bibliographic Links | [Context Link]

37. Scherphof G, Roerdink F, Dijkstra J, Ellens H, De Zanger R, Wisse E. Uptake of liposomes by rat and mouse hepatocytes and Kupffer cells. Biol Cell 1983;47:47-58. Link Resolver | Bibliographic Links | [Context Link]

38. Gillis P, Koenig SH. Transverse relaxation of solvent protons induced by magnetized spheres: Application to ferritin, erythrocytes, and magnetite. Magn Reson Med 1987;5:323-345. Link Resolver | Bibliographic Links | [Context Link]

39. Kennan RP, Zhong J, Gore JC. Intravascular susceptibility contrast mechanisms in tissues. Magn Reson Med 1994;31:9-21. Link Resolver | Bibliographic Links | [Context Link]

40. Bouwens L, Baekeland M, De Zanger R, Wisse E. Quantitation, tissue distribution and proliferation kinetics of Kupffer cells in normal rat liver. Hepatology 1986;6:718-722. Link Resolver | Full Text | Bibliographic Links | [Context Link]

41. Sleyster EC, Knook DL. Relation between localization and function of rat liver Kupffer cells. Lab Invest 1982;47:484-490. Link Resolver | Bibliographic Links | [Context Link]

42. Roitt IM. In: Essential immunology. Oxford, England: Blackwell Scientific Publications, 1994. [Context Link]

43. Weisskoff RM, Zuo CS, Boxerman JL, Rosen BR. Microscopic susceptibility variation and transverse relaxation: Theory and experiment. Magn Reson Med 1994;31:601-610. Link Resolver | Bibliographic Links | [Context Link]

44. Colet JM, Pierart C, Seghi F, Gabric I, Muller RN. Intravascular and intracellular hepatic relaxivities of superparamagnetic particles: An isolated and perfused organ pharmacokinetics study. J Magn Reson Imaging. In press. [Context Link]

45. Majumdar S, Zoghbi SS, Gore JC. The influence of pulse sequence on the relaxation effects of superparamagnetic iron oxide contrast agents. Magn Reson Med 1989;10:289-301. Link Resolver | Bibliographic Links | [Context Link]

KEY WORDS: Liposomal Gd-HP-DO3A; liposome, size, composition; liver contrast enhancement; dipolar relaxation; susceptibility effects

IMAGE GALLERY

Select All

Export Selected to PowerPoint

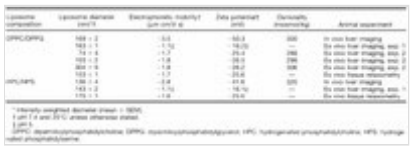

Table 1

$$\ln C = \ln C_0 - kt$$

Equation 1

$$t_{1/2} = \ln 2/k$$

Equation 2

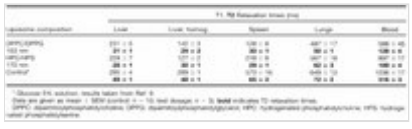

Table 2

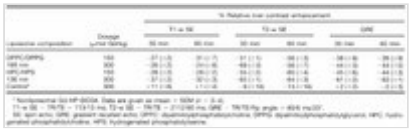

Table 3

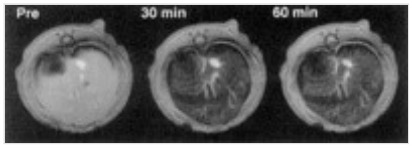

Figure 1

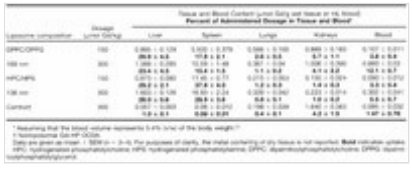

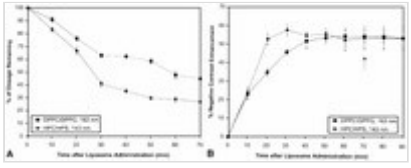

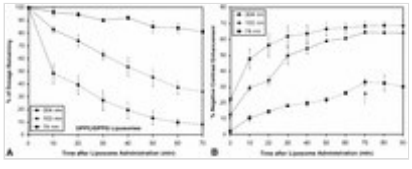

Table 4 Figure 2 Figure 3

Liposome size	Liver content (μmol Gd/g wet liver) **Liver uptake (Percent of administered dosage)**	P/NP Gd ratio*
74 nm	0.331 ± 0.019 **13.0 ± 2.4**	4.8
103 nm	1.659 ± 0.157 **56.7 ± 5.6**	0.20
304 nm	2.767 ± 0.290 **83.9 ± 6.7**	3.4×10^{-3}

* $n = 1$. Data are given as mean ± SEM ($n = 2$). **Bold** indicates liver uptake.
For purposes of clarity, the metal content/g of dry tissue is not reported.
P/NP Gd ratio: ratio of the Gd content in parenchymal vs non-parenchymal cell fractions.

Table 5

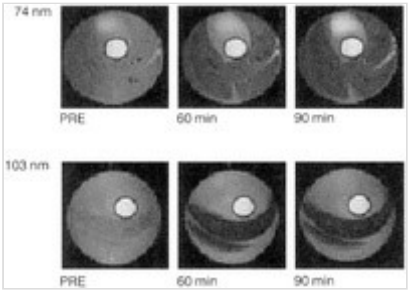

Figure 4

Back to Top

OvidUI_04.12.01.011, SourceID 7b25af8fc0e3e45cb065d02c59c55fad501d9039